

Supplementary Material (ESI) for Chemical Communications
This journal is (c) The Royal Society of Chemistry 2012

Supporting Information

Facile synthesis of porous MnO/C nanotubes as a high capacity anode material of lithium ion batteries

Gui-Liang Xu,^a Yue-Feng Xu,^a Hui Sun,^b Fang Fu,^a Xiao-Mei Zheng,^a Ling Huang,^a Jun-Tao Li,^a Shi-He Yang^b and Shi-Gang Sun^{*a}

^a State Key Laboratory of Physical Chemistry of Solid Surfaces, Department of Chemistry, College of Chemistry and Chemical Engineering, School of Energy Research, Xiamen University, Xiamen 361005, China

^b Department of Chemistry, The Hong Kong University of Science and Technology, Clear Water Bay, Kowloon, Hong Kong

*Corresponding author Email: sgsun@xmu.edu.cn

Experimental

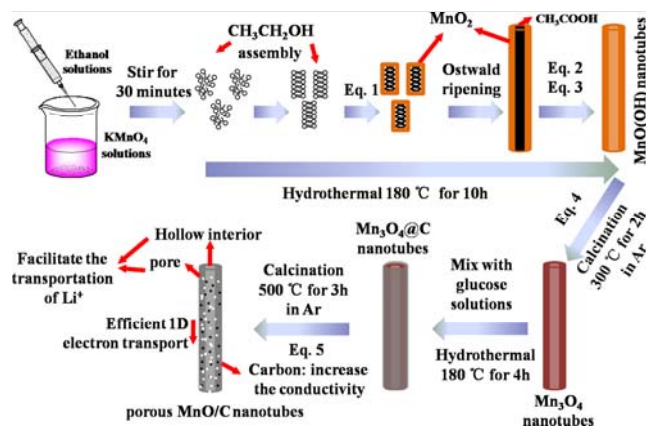
Materials preparation: the synthesis procedure of porous MnO/C nanotubes is illustrated in Scheme 1. In a typical synthesis of MnO(OH) nanotubes, 0.8 g KMnO₄, 1.5 mL ethanol and 45 ml deionized water were mixed under magnetic stirring. After 30 minutes stirring, the mixture was transferred and sealed in a 50 ml Teflon-lined autoclave, heated at 180 °C for 10 h, and finally cooled to room temperature. And then the as-prepared MnO(OH) nanotubes was subjected to heat treatment in high purity argon atmosphere at 300 °C for 2 h to obtain Mn₃O₄ nanotubes. For carbon coating, 0.15 g glucose and 0.2 g Mn₃O₄ nanotubes were added into 20 mL deionized water were mixed under magnetic stirring and then transferred and sealed in a 50 ml Teflon-lined autoclave, heated at 180 °C for 4 h. Finally, the product was heated in high purity argon atmosphere at 500 °C for 4 h to obtain generate porous MnO/C nanotubes.

Materials Characterization: The morphologies and structures of the as-prepared samples were characterized by field emission scanning electron microscopy (HITACHI S-4800), transmission electron microscopy (FEI Tecnai-F30 FEG) and powder X-ray diffraction (XRD, Philips X'pert Pro Super X-ray diffractometer, Cu K α radiation) measurements. The content of carbon was measured by elemental analysis on the instrument of Vario Elemental III (Elementar Co., German). The specific surface areas of the as-prepared samples were measured by the Brunauer–Emmett–Teller (BET) method using nitrogen adsorption and desorption isotherms on a Tristar3000 system. Raman experiment was performed on XploRA (HORIBA) using 532 nm excitation line with a laser power about 0.1 mW on the sample surface.

Electrochemical Measurements: The electrodes were prepared by spreading a mixture of 75wt % MnO active material, 15wt % acetylene black and 10wt % LA132 on to a copper foil current collector. The as-prepared electrodes were dried at 80 °C in vacuum oven for 24 h and pressed under 10 MPa. Electrochemical properties of the electrodes were measured by assembling them into coin cells (type CR2025) in an argon-filled glove box with water and oxygen contents less than 0.5 ppm. Li

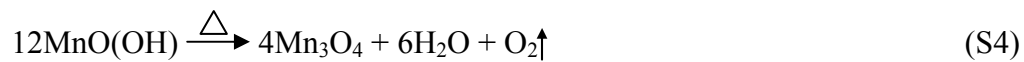
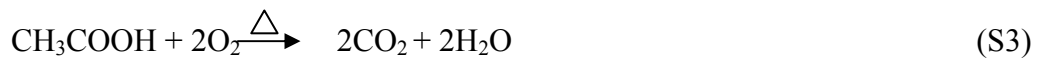
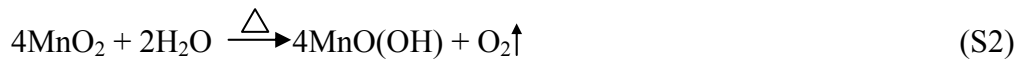
foil was used as the counter electrode and polypropylene (PP) film (Celgard 2400) as the separator. The electrolyte was made from LiPF_6 (1M) in a mixture of ethylene carbonate (EC)/ dimethyl carbonate (DMC)/ diethyl carbonate (DEC) in a volume ratio of 1:1:1 with 2 wt % vinylene carbonate (VC) as additive. The cells were galvanostatically charged and discharged in a battery test system (LAND-V34, Land Electronic Co., Ltd., Wuhan) for a cut-off voltage of 0.02-3.0 V (vs. Li/Li^+) at room temperature. Cyclic voltammetry (CV) was performed on CHI 660C electrochemical workstation (shanghai) using coin cell at a scan rate of 0.1 mV s^{-1} from 0.02 V to 3.0 V.

1. Scheme for the formation of porous MnO/C nanotubes



Scheme 1 The formation process of porous MnO/C nanotubes

2. Equations for the formation of porous MnO/C nanotubes



3. SEM images of the products at different hydrothermal reaction time

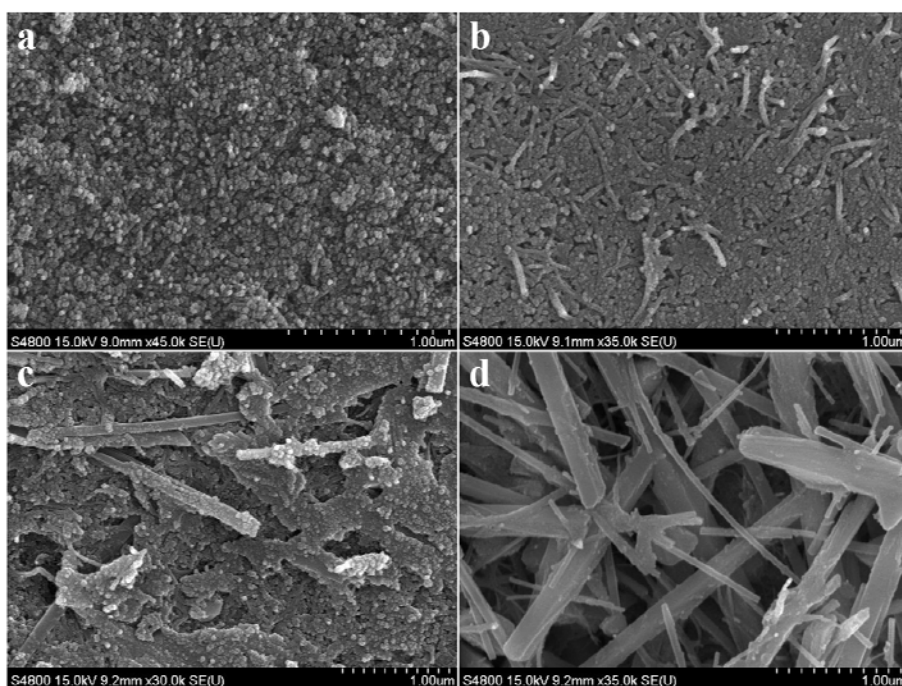


Fig. S1 SEM images of the products at different hydrothermal reaction time: (a) 0.5 h; (b) 1 h; (c) 1.5 h and (d) 2 h.

4. Morphology characterization of the MnO(OH) nanotubes

The crystallographic structure and phase purity of the as-synthesized MnO(OH) nanotubes are examined by X-ray powder diffraction (XRD). The XRD pattern (Fig. S2a) can be indexed to the monoclinic MnO(OH) with space group of P21/c, which is in good accordance with the standard XRD pattern of MnO(OH) (JCPDF no. 01-088-0649). The as-prepared MnO(OH) nanotubes were also confirmed by SEM image in Fig. S2b. Numerous 1D nanostructures with tubular morphology were formed in high yield, most of which are straight and have an average diameter of 352 nm (Fig. S2c) and lengths of several micrometers. Transmission electron microscopy (TEM) image in Fig. S2d clearly reveal the tubular structure of the as-prepared MnO(OH) nanotubes.

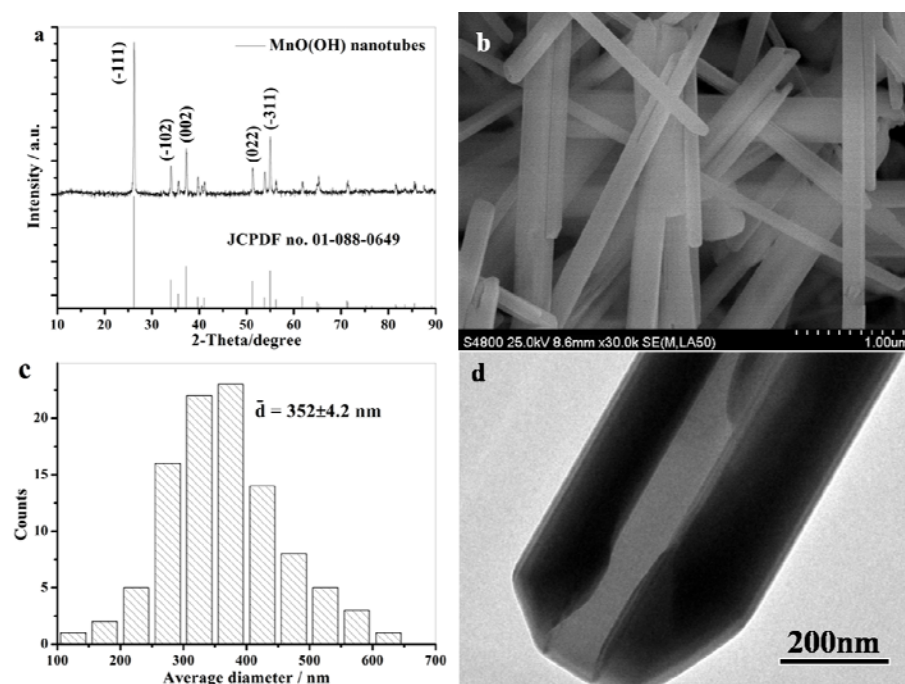


Fig. S2 (a) XRD pattern, (b) SEM image, (c) diameter histogram and (d) TEM image of MnO(OH) nanotubes.

5. N₂ adsorption/desorption measurements of the porous MnO/C nanotubes.

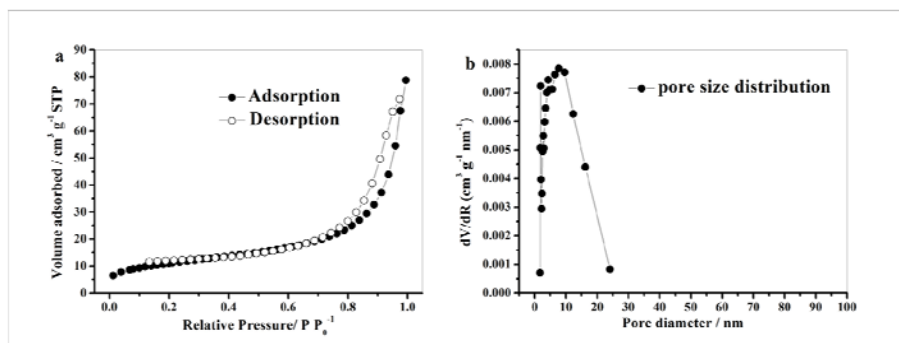


Fig. S3 (a) N₂ adsorption/desorption isotherms and (b) pore size distribution of porous MnO/C nanotubes.

6. Characterization of carbon in the porous MnO/C nanotubes

In the XRD pattern of porous MnO/C nanotubes (Fig. 2d), no diffraction peaks from crystalline carbon (25.7° and 44.2°) are observed, while a weak and broad peak from amorphous carbon (10° to 25°) can be seen clearly as illustrated in Fig. 4a. The Raman spectrum of porous MnO/C nanotubes is illustrated in Fig. S4b. Two broad peaks attributing to the typical disordered band (D band) (1377 cm^{-1}) and graphene band (G band) (1597 cm^{-1}) of carbon are observed. The peaks are very broad, indicating the carbon structure is not well crystallized. Moreover, the intensity ratio of the D band to the G band (I_D/I_G), standard of the graphitization degree, is calculated. The I_D/I_G value of porous MnO/C nanotubes is 0.81, which is much higher than the I_D/I_G value (0.09) of fully graphitized carbon.^{s1, s2} This indicates that the carbon in the porous MnO/C nanotubes is in an amorphous state.

As the content of carbon in the porous MnO/C nanotubes is only 3.2wt%, the thickness of carbon layer is very thin (ca. 0-2 nm), as shown in the TEM image below (Fig. S4c). While when the content of carbon was increased to 20wt%, the thickness of carbon layer could be increased to ca. 30 nm in our experiment (Fig. S4d).

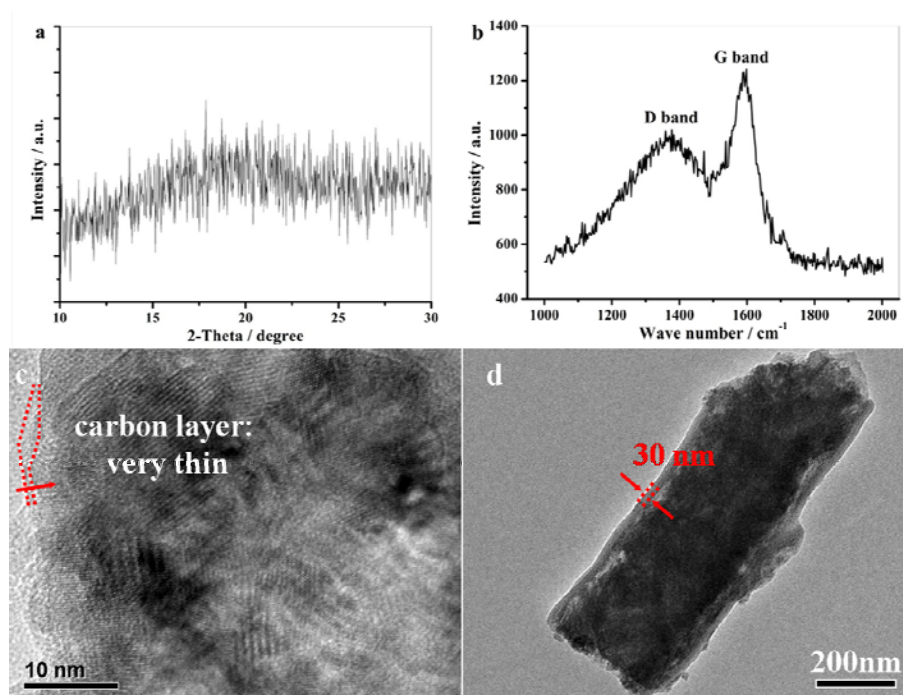


Fig. S4 (a) magnified XRD pattern of porous MnO/C nanotubes from 10° to 30° ; (b) Raman spectrum and (c) HR-TEM image of porous MnO/C nanotubes; (d) TEM image of MnO/C nanotubes with 20wt% of carbon.

7. SEM elemental mapping images of the porous MnO/C nanotubes.

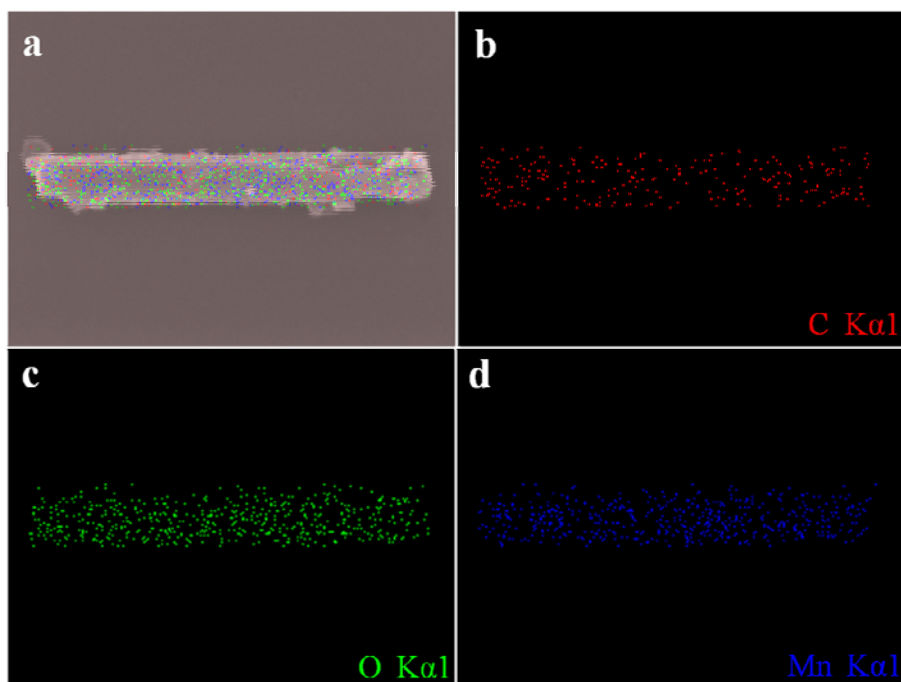


Fig. S5 SEM elemental mapping images of (a) carbon (red), oxygen (green) and manganese (blue), (b) carbon, (c) oxygen and (d) manganese in the porous MnO/C nanotubes.

8. Cyclic voltammograms of porous MnO/C nanotubes at a scan rate of 0.1 mV s⁻¹.

Fig. S6 displays the cyclic voltammograms of porous MnO/C nanotubes at a scan rate of 0.1 mV s⁻¹. In the first cycle, a weak and broad peak around 1.5-2.0V appeared and disappeared in the subsequent cycles, which is ascribed to the decomposition of electrolytes to form SEI layer. A pronounced cathodic peak is observed from 0.3V to 0.02V, which is attributed to the conversion reaction between MnO and lithium to form manganese nanocrystals well dispersed in Li₂O matrix. This peak is shifted to a positive voltage i.e. 0.25V due to reduction of MnO and the well disperse of manganese metallic nanograins in the Li₂O matrix after the first cycle. An anodic peak appears at ca. 1.3V, corresponding to the reverse process of conversion reaction. Moreover, the peaks of the 4th cycle nearly overlap with that of the 5th cycle, indicating a good cycle performance of the porous MnO/C nanotubes.

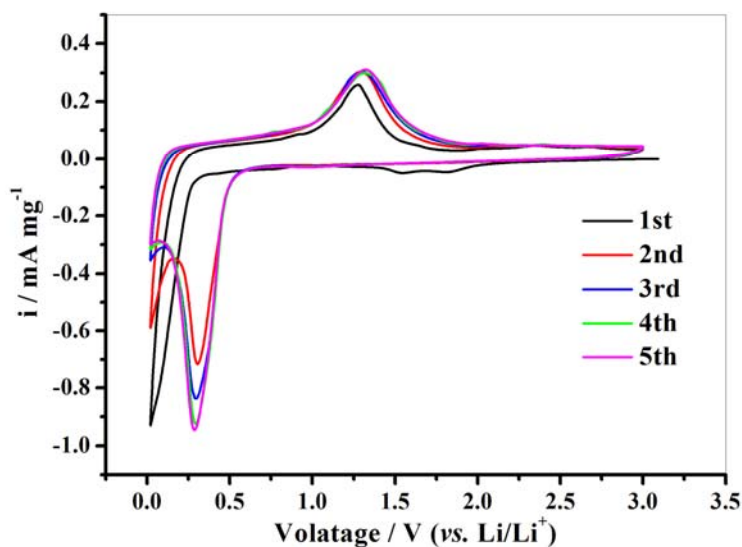


Fig. S6 Cyclic voltammograms of the porous MnO/C nanotubes at a scan rate of 0.1 mV s⁻¹ between 0.02-3.0V.

9. SEM images of commercial MnO particles.

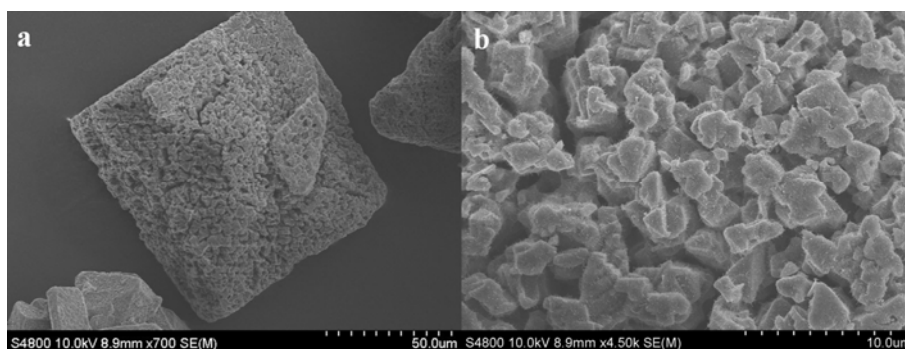


Fig. S7 SEM images of commercial MnO particles in (a) low and (b) high magnification.

10. Morphology characterization of the porous MnO/C nanotubes electrode after charge/discharge.

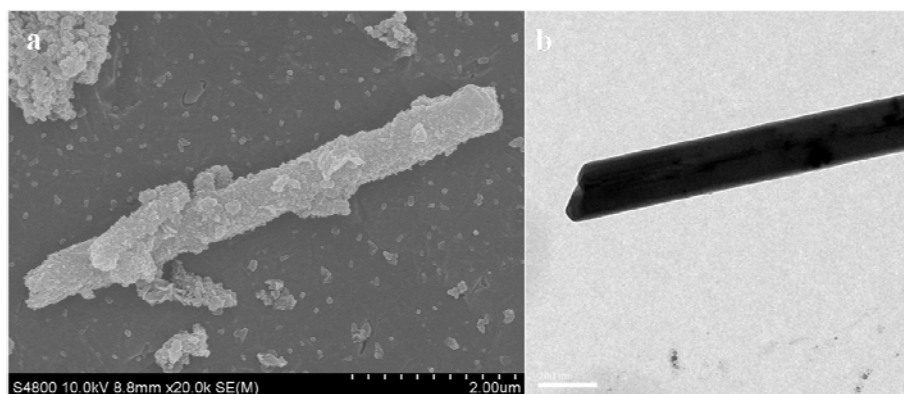


Fig. S8 (a) SEM image and (b) TEM image of porous MnO/C nanotubes electrode after 100 cycles of charge/discharge at rate of 0.13C.

11. Elemental analysis of carbon in the porous MnO/C nanotubes conducted on Vario Elemental III (Elementar Co., German).

Table S1 Elemental analysis result of the porous MnO/C nanotubes

Wght. [mg]	C/N Ratio	Content [%]	Peak Area
3.7200	82.35	N:0.038	101
		C:3.151	3181
		H:0.426	743

References:

- S1. A. Cuesta, P. Dhamelincourt, J. Laureyns, A. Martinezalonso and J. M. D. Tascon, *Carbon*, 1994, **32**, 1523-1532.
- S2. Y. He, L. Huang, X. Li, Y. Xiao, G. L. Xu, J. T. Li and S. G. Sun, *J Mater Chem*, 2011, **21**, 18517-18519.